Differential Expression Profiles of Long Noncoding RNA and mRNA in Dexamethasone-Induced Apoptosis of Human Bone Marrow Mesenchymal Stem Cells

Tao Li
affiliated hospital of qingdao university
Yingxing Xu
the Affiliated Hospital of Qingdao University
Yingzhen Wang
the affiliated hospital of qingdao university
Yaping Jiang (jyp6817@163.com)
The Affiliated Hospital of Qingdao University

Research

Keywords: MSCs, Gene expression, Long noncoding RNA, Apoptosis, Dexamethasone

Posted Date: June 18th, 2020

DOI: https://doi.org/10.21203/rs.3.rs-34807/v1

Version of Record: A version of this preprint was published on January 6th, 2021. See the published version at https://doi.org/10.1186/s13287-020-02040-8.

Abstract

Background

Abnormalities in apoptosis, cell cycle, and proliferation of human bone marrow mesenchymal stem cells (hBMSCs) significantly impact bone metabolism and remodeling, and thereby cause various skeletal disorders. Long-term exposure to a high dosage of dexamethasone (Dex) induces apoptosis and inhibits proliferation of mesenchymal stromal cells (MSCs), which are probably the primary causes of osteoporosis (OP) and steroid-induced osteonecrosis of the femoral head (SONFH). However, to date, the exact mechanisms of Dex-induced apoptosis of BMSCs are still poorly defined.

Methods

A microarray was used to identify differentially expressed lncRNA and mRNA in Dex-induced apoptosis of hBMSCs, and bioinformatics was used to further explore the role of these differentially expressed lncRNAs and mRNAs by the coding and noncoding (CNC) network. Furthermore, validation of the microarray results was performed by quantitative real-time PCR (qRT-PCR) analysis.

Results

The microarray analysis identified a total of 137 differentially expressed mRNA (90 up-regulated and 47 down-regulated) and 90 differentially expressed lncRNA (61 up-regulated and 29 down-regulated) in Dex-induced apoptosis of hBMSCs. The differentially expressed mRNA and lncRNA were associated with the regulation of cell apoptosis. Meanwhile, several signaling pathways involved in the regulation of cell apoptosis, including mTOR signaling pathway, Ras signaling pathway, HIF-1 signaling pathway, NF-kappa B signaling pathway, and TGF-beta signaling pathway, also were identified in interaction net of the significant pathways (Path-Net) analysis. Furthermore, the CNC network further identified 78 core regulatory genes involved in the regulation of apoptosis. Besides, validation by qRT-PCR of the key differentially expressed mRNA and lncRNA, reported to be closely related to cell apoptosis, confirmed the reliability of the microarray dataset.

Conclusions

Collectively, we utilized microarray to identify differentially expressed lncRNA and mRNA in Dex-induced apoptotic hBMSCs, and bioinformatics to explore the interaction between the differentially expressed genes. This study demonstrates the molecular mechanisms of Dex-induced apoptosis of hBMSCs and provides a new research direction for the study of the pathogenesis of steroid-induced osteonecrosis of femoral head.

1. Introduction

Human bone marrow mesenchymal stem cells (hBMSCs) have the capacity of self-renewal and differentiation into osteocytes, osteoblasts, adipocytes, chondrocytes, and other embryonic lineages [1]. Therefore, abnormal apoptosis, cell cycle arrest, and proliferation of hBMSCs have a significant impact on bone metabolism and remodeling and act as a trigger for various skeletal disorders [2, 3].

Dexamethasone (Dex) is one of the most commonly used glucocorticoid (GC) drugs. Long-term use of Dex is limited by several adverse effects including, bone loss, low bone mass, risk of fragility fracture, and osteonecrosis [4]. Notably, many reports have demonstrated dose and duration dependent variability in Dex induced responses in mesenchymal stromal cells (MSCs) depending on the concentration and exposure time[5, 6]. For example, whereas short and low dosage of Dex treatment on MSCs stimulated osteogenesis[7, 8], long-term exposure to high dosage (10^{-6} mol/L) induced apoptosis and inhibited proliferation of BMSCs[5, 6]-probable mechanisms in osteoporosis (OP) and steroid-induced osteonecrosis of the femoral head (SONFH). However, to date, the exact mechanisms of Dex-induced apoptosis of BMSCs are still poorly defined. Apoptosis of BMSCs is related to many factors, including not only the cell-cycle arrest and proliferation inhibition but also the regulation of gene transcription and signaling pathways[9–12].

Long noncoding RNAs (lncRNAs) are a class of non-protein-coding genes which are more than 200 nucleotides in length[13]. Emerging evidence has suggested that lncRNAs participate in a wide variety of cellular processes including, apoptosis, proliferation, migration, and differentiation of BMSCs[14, 15]. Functionally, lncRNAs regulate gene expression via interfering with DNA, mRNA, or protein[13].

This present study aims we utilized microarray and bioinformatics to identify differentially expressed lncRNA and mRNA in Dex-induced apoptosis of hBMSCs and to explore the role of these differentially expressed lncRNAs and mRNAs by predicting the interactions between coding and noncoding genes. Furthermore, we validated the microarray results by quantitative real-time PCR (qRT-PCR).

2. Material And Methods

2.1. Isolation, Culture, and Characterization of hBMSCs

2.1.1. Isolation and culture of hBMSCs

The present study was approved by the Ethics Committee of the Affiliated Hospital of Qingdao University (Qingdao, China). Bone marrow sample was collected from three patients with the fracture of the femoral neck (age 45, 47, and 52) during total hip arthroplasty (THA) surgery in the Department of Orthopedics at Qingdao University Affiliated Hospital. All donors gave signed informed consent. Cells were isolated and purified from the bone marrow tissue by density gradient centrifugation as previously described[16], and then were cultured in Dulbecco modified Eagle's medium (DMEM, Solarbio, Beijing, China) containing 10%

(v/v) fetal bovine serum (FBS, Gibco, Thermo Scientific, Australia) and 100 units/ml penicillin-streptomycin (Solarbio, Beijing, China) at 5% CO_2 and 37 °C. Cells were passaged in a 1:2 ratio at 90% confluency. Cells at passage three were used for all downstream experiments.

2.1.2. Phenotypes of hBMSCs

Flow cytometric analysis was used to assess hBMSCs surface marker expression on the Apogee A50-MICRO flow cytometer (Apogee, UK) according to the following procedure. Briefly, cells were digested with trypsin, centrifugated, and resuspended in cold phosphate-buffered saline (PBS) containing 1% FBS. After adjusting the concentration to 1×10^6 cells/ml, the cell suspension was incubated with following antibodies: 20 μL of anti-CD34PE, 20 μL of anti-CD45PE, 5 μL of anti-CD73-FITC, 2 μL of CD90FITC (BD Biosciences, USA), respectively, for 30 minutes in dark at 37 °C. Following washing with cold PBS three times, 100 μL of single-cell suspension was used for flow cytometric analysis. Untreated cells were utilized as a negative control.

2.1.3. Osteogenic and adipogenic differentiation of hBMSCs

The osteogenic and adipogenic differentiation of hBMSCs were evaluated by using a differentiation medium (Fuyuanbio, Shanghai, China) as per the manufacturer's instructions. Cells at 60% and 90% confluency were, cultured in osteogenic and adipogenic induction medium, respectively. Osteogenic differentiation of hBMSCs was assessed by alkaline phosphatase (ALP) staining (Solarbio, Beijing, China) after 7 days, and adipogenic differentiation was assessed by oil red O staining (Solarbio, Beijing, China) after 14 days.

2.2. Dex-induced apoptosis of hBMSCs

2.2.1. Treatment of hBMSCs with Dex

The complete medium is. hBMSCs were cultured in complete DMEM containing 10% FBS and 100 units/ml penicillin-streptomycin with 10^{-6} mol/L Dex (Dex-induced group, Dex) or without Dex (control group, Control).

2.2.2. Assessment of the morphology of apoptotic cells

Cells at passage 3 were grown in 24-well plates and treated as mentioned above. After 7 days, chromatin dye Hoechst 33342 Kit (Solarbio, Beijing, China) was used to assess the morphology of apoptotic cells as per the manufacturer's instructions. Apoptotic cells were identified and counted under a fluorescent microscope for following morphological characteristics, such as chromatic agglutination, karyopyknosis, and nuclear fragmentation. Triplicate samples were analyzed in each group with three replicates per experiment.

2.2.3. Flow cytometric analysis for apoptosis

Cells at passage 3 were grown in 24-well plates and treated as mentioned above. After 7 days, Annexin V-PE/7-AAD Kit (BD Biosciences, USA) was used to analyze the percentage of apoptotic cells by Apogee

A50-MICRO flow cytometer (Apogee, UK) as the manufacturer's manuals described, and at least 10^4 cells were analyzed for each sample. Samples in triplicate were analyzed in each group with three replicates per experiment.

2.3. Microarray

After treatment for 7 days, total RNA from hBMSCs in the two groups was extracted using the RNAiso plus kit (Takara Bio Inc., Kusatsu, Japan) as per the manufacturer's instructions. The purity and concentration of RNA were assessed by OD260/280 on a spectrophotometer (NanoDrop ND-1000). Total RNA was reverse-transcribed into cDNA, which was labeled with a fluorescent dye (Cy5 and Cy3-dCTP) and hybridized with the Agilent human lncRNA + mRNA Array V4.0 designed with four identical arrays per slide (4 × 180K format). The microarrays were washed and then scanned using a G2565CA Microarray Scanner (Agilent). The lncRNA + mRNA array data were analyzed for data summarization, normalization, and quality control by using the GeneSpring software V13.0 (Agilent). The threshold values, a fold change ≥ 2.0 or ≤ 2.0 and P values (T-test) < 0.05, were used to select the differentially expressed lncRNA and mRNA. Three parallel replicates were made in the experiment.

2.4. Bioinformatic Analysis

DAVID Bioinformatics Resources 6.8 (https://david.ncifcrf.gov/) was used to conduct Gene ontology (GO) and pathway enrichment analysis. GO enrichment analysis was performed to identify the functions of the differentially expressed genes between the two groups, including biological process, cellular component, and molecular function. Pathway enrichment analysis was performed using Reactome, KEGG, PID, PANTHER, BioCarta, and BioCyc. Furthermore, the coding-non-coding gene co-expression (CNC) network was constructed based on the correlation analysis between the mRNA and lncRNA expression (Pearson correlation coefficients > 0.99 or ≤ 0.99). A P value < 0.05 was considered statistically significant.

2.5. Quantitative Real-Time PCR (qPCR)

Differentially expressed mRNA and lncRNA were selected randomly to confirm the results of microarray assays by qRT-PCR. Total RNA was obtained from hBMSCs in the two groups using the RNAiso plus kit (Takara Bio Inc., Kusatsu, Japan), and then reverse transcribed into cDNA by PrimeScript RT reagent kit (Takara Bio Inc., Kusatsu, Japan). The qRT-PCR was performed on a Roche LightCycler 480 Detection System (Roche, Switzerland), using the SYBR Premix Ex Taq □ kit (Takara Bio Inc., Kusatsu, Japan) as per the manufacturer's instructions. All the forward and reverse primers for each gene were provided by the Ribobio Corporation (Guangzhou, China). Relative expression of each gene was evaluated by the $2^{-\triangle\triangle Ct}$ method and normalized to GAPDH. Triplicate samples were analyzed in each group with three parallel replicates in each experiment.

2.6. Statistical Analysis

The SPSS 19.0 software (IBM, Armonk, NY, USA) was used to conduct statistical analysis. All data are presented as means ± SD, and P-value < 0.05 was considered as statistical significance. Charts were made in GraphPad Prism 8 software (GraphPad, CA, USA).

3. Results

3.1. Identification of hBMCSs

After two to three passages, cultured cells exhibited the characteristics of fibroblast-like and spindle-shaped morphology homogeneously. (Fig. 1A). ALP and oil red O staining confirmed osteogenic as well as adipogenic differentiation capability of the cells (Fig. 1B-1D). Phenotyping of hBMSCs by flow cytometry showed that these cells were positive for CD73 (95%), CD90 (93.1%) (two cell surface markers for marrow-derived stem cells), but negative for CD34 (97.6%) and CD45 (96.5%) (two specific cell surface markers for hematopoietic cells) (Fig. 1E).

3.2. Dex-induced apoptosis of hBMSCs

Hoechst 33342 staining showed apoptotic characteristics such as chromatic agglutination, karyopyknosis, and nuclear fragmentation, after continuous exposure to 10^{-6} mol/L Dex for 7 days (Fig. 2A). Moreover, flow cytometry analysis of Annexin V-PE/7-AAD double-staining demonstrated that 10^{-6} mol/L Dex significantly increased the percentage of apoptotic cells (Fig. 2B). Based on the above results, 10^{-6} mol/L Dex significantly induced apoptosis of hBMSCs after treatment for 7 days.

3.3. Differential expression profile of mRNA in Dex-induced apoptosis of hBMSCs and bioinformatics

The microarray identified a total of 137 differentially expressed mRNA in Dex treated hBMSCs compared with the control (FC $\geq$ 2, *P*-value < 0.05), out of which 90 were up-regulated, and 47 were down-regulated (Fig. 3A1-A2, Supplemental file 1).

GO enrichment analysis revealed that the differentially expressed mRNA were enriched in many biological processes including regulation of cell cycle, cell division, cell proliferation, cytokine-mediated signaling pathway, and cGMP-mediated signaling (*P*-value < 0.05) (Fig. 3B1), which are closely related to apoptosis [17, 18]. In the molecular function category, enrichment was seen in procollagen-proline 4-dioxygenase activity, enzyme binding, protein binding, carbohydrate derivative binding, kinase binding, cytokine binding (*P*-value < 0.05) (Fig. 3B2). In the cellular component, they were enriched in midbody, condensed chromosome kinetochore, kinetochore, spindle, intracellular organelle lumen, especially BIM-BCL-2 complex, which plays a significant role in promoting apoptosis [19] (*P*-value < 0.05) (Fig. 3B3).

Moreover, pathway enrichment analysis identified a total of 71 significantly differential signaling pathways (39 from Reactome, 13 from KEGG, 10 from PID, 3 from PANTHER, 4 from BioCarta, 2 from BioCyc). Among the top 30 signaling pathways, most of them were related to the regulation of apoptosis[20–22], such as cell cycle, signaling by Rho GTPases, polo-like kinase-mediated events, Cyclin B2 mediated events, and cytokine-cytokine receptor interaction (*P*-value < 0.05) (Fig. 3C).

3.4. Interaction net of significant pathways (Path-Net) of the differentially expressed mRNA

A Path-Net of the differentially expressed mRNA was constructed on the KEGG database to identify the comprehensive interactions between the significant pathways. Our results showed upregulation of the signaling pathways mediated by mTOR, thyroid hormone, Ras, insulin resistance, HIF-1, and glucagon. By contrast, signaling mediated through NF-kappa B, TGF-beta, and Calcium, and pathways regulating pluripotency of stem cells were downregulated (Fig. 4). Among these, mTOR, Ras, HIF-1, NF-kappa B, and TGF-beta signaling pathways have been confirmed to be associated with apoptosis [23–27].

3.5. Differential expression profile of lncRNA in Dex-induced apoptosis of hBMSCs

A total of 90 differentially expressed lncRNA were detected in Dex-induced apoptosis of hBMSCs (FC ≥ 2, *P*-value < 0.05); of these, 61 were upregulated and 29 were downregulated, including 41 intergenic, 4 intronic, 5 divergent, 21 antisense, 17 uncategorized and 2 unpublished lncRNA (Fig. 5A1-A2, Supplemental file 2).

Furthermore, pathway enrichment analysis revealed a total of 6 significantly differential signaling pathways (4 from Reactome, 1 from KEGG, 1 from PANTHER), such as inactivation of Cdc42 and Rac, signaling by Robo receptor, Rho GTPase cycle and PDGF signaling pathway (*P*-value < 0.05) (Fig. 5B). According to the previous studies, these signaling pathways have been reported to be associated with the regulation of apoptosis, cell cycle, and cell proliferation[28–31].

3.6. CNC network analysis of key differentially expressed mRNA and lncRNA

A CNC network was constructed by the correlation analysis, to evaluate the interactions between the differentially expressed lncRNA and mRNA. Our analysis identified a total of 78 core regulatory genes, including 47 mRNA and 31 lncRNA (Supplemental file 3). As shown in Fig. 6, 15 lncRNAs were correlated with one mRNA, whereas the others were correlated with two or more mRNA. In particular, an interaction network was identified from lncRNA (XLOC_011523) to mRNA (CDKN3, E2F7, and IQGAP3), involving 21 mRNA and 8 lncRNA. Moreover, some key mRNA were identified, such as GINS4, CIT, CDK1, SAMHD1, and CDH11, which were reported to be closely associated with the regulation of cell proliferation and apoptosis [32–36].

3.7. Validation by qRT-PCR

We randomly selected 6 differentially expressed mRNA (3 up-regulated and 3 down-regulated), and 4 differentially expressed lncRNA (3 up-regulated and 1 down-regulated) based on previous reports to confirm the reliability of microarray data and facilitate downstream analysis (Table 1). Consistent with

the microarray data, qRT-PCR validated the upregulation of the GINS complex subunit 4 (GINS4), citron rho-interacting serine/threonine kinase (CIT) and cyclin-dependent kinase 1 (CDK1), and the down-regulation of BCL2-like 11 (BCL2-L11), SAM domain and HD domain 1 (SAMHD1), and cadherin 11 (CDH11) (Fig. 7A). Besides, the following lncRNAs were up-regulated: STXBP5-AS1, IFNG-AS1, and MIR210HG, whereas ZFHX4-AS1 was down-regulated (Fig. 7B).

Table 1
The details of differentially expressed mRNA and lncRNA selected for confirmation in Dex-induced apoptosis of hBMSCs

Gene name	Gene type	Regulation	Microarray (FC abs)	Primer sequence (5′-3′)
IFNG-AS1	lncRNA	Up	2.462	F: GACAACATGGTACATGTGGCTAG
				R: CCTCGGTTGCTTTGATTACACA
STXBP5-AS1	lncRNA	Up	3.621	F: GAGATTTAGGTGGGGACGCTGC
				R: AGGGACTTGCCTTGTCGCTGAT
MIR210HG	lncRNA	Up	8.502	F: GCTTGGTAGAGTGTCACGCC
				R: CATCTGACCGAGCCAGTTTG
ZFHX4-AS1	lncRNA	Down	2.975	F: GCGCTCAGAAGTTTACAAGG
				R: CTCTAGCTGAGTCTTCTGCT
CDK1	mRNA	Up	3.105	F: AGCCGGGATCTACCATACCC
				R: TCGAGAGCAAATCCAAGCCA
CIT	mRNA	Up	2.648	F: ATATGGAGCGCGGAATCCTTT
				R: TCAGCTATGGTGTCGGAATACT
GINS4	mRNA	Up	2.671	F: TCAAGCCTGTAATCCCAGCA
				R: GTTCAAGCGATTCTCCTGCC
BCL2-L11	mRNA	Down	2.257	F: GCATCATCGCGGTATTCGGT
				R: TCTGGTAGCAAAAGGGCCAG
CDH11	mRNA	Down	3.203	F: CCGTACAGTTGGTGGAAGGG
				R: ACGTGTACTGGGCTCTCTCT
SAMHD1	mRNA	Down	2.440	F: AGTATGTGGGTGAGACGCAG
				R: GGAAGAGATTCATAGTCCTCCCTT

CIT = citron rho-interacting serine/threonine kinase; CDK1 = cyclin-dependent kinase 1; GINS4 = GINS complex subunit 4; BCL2-like 11 = B-cell lymphoma 2-Like 11; CDH11 = cadherin 11; SAMHD1 = SAM domain and HD domain 1; FC abs = fold change absolute value; F = forward; R = reverse; lncRNA = long noncoding RNA; Dex = dexamethasone; hBMSCs = human bone marrow mesenchymal stem cells.

4. Discussion

Induction of multilineage differentiation of MSCs by Dex into osteoblasts, adipocytes, skeletal muscle cells, and chondroblasts is accepted widely[1]. However, this diverse induction of Dex in MSCs is

depended on the concentration and exposure time[5–8]. Shifting the focus from multilineage differentiation of MSCs, recent studies are paying more attention to the pro-apoptotic effect of Dex. It was reported that long-term exposure to a high dosage of Dex (10^{-6} mol/L) induced apoptosis and inhibited proliferation of BMSCs[5, 6], which may contribute to the pathogenesis of skeletal and metabolic disorders, including OP, SONFH, fragility fracture. Nevertheless, the exact mechanism of Dex-induced apoptosis of MSCs remains equivocal, despite reports that Dex can regulate gene expression of MSCs[37].

Emerging evidence has revealed that a large number of signaling pathways, such as PI3K/Akt/mTOR[23], RAF-MEK-MAPK/ERK[38], NF-kB[26] and p53-dependent signaling pathway[39], are implicated in apoptosis. These signaling pathways are regulated by a variety of transcripts, including coding and noncoding RNAs. The lncRNA is a kind of noncoding RNA with a length ofmore than 200 nucleotides and has been reported to regulate apoptosis, proliferation, migration, and differentiation of MSCs by interfering with DNA, mRNA, or protein[40–42]. However, it is still unclear which crucial genes are involved in the apoptosis of Dex-induced MSCs.

Here, we utilized microarray to identify differentially expressed lncRNA and mRNA in Dex-induced apoptosis in hBMSCs and identified 137 differentially expressed mRNA (90 up-regulated and 47 down-regulated). The GO enrichment analysis demonstrated that these differentially expressed mRNA were enriched in the regulation of cell cycle, cell division, cell proliferation- processes closely related to apoptosis. Moreover, pathway enrichment analysis identified a total of 71 significantly differential signaling pathways mainly involved in the cell cycle, signaling by Rho GTPases, polo-like kinase-mediated events, Cyclin B2 mediated events, and cytokine-cytokine receptor interaction were closely related to the regulation of apoptosis[20–22]. Furthermore, Path-Net analysis highlighted signaling pathways mediated by mTOR, Ras, HIF-1, NF-kappa B, and TGF-beta may play critical roles in Dex-induced apoptosis of hBMSCs; consistent with previous reports[23–27]. Notably, many signaling pathways pointed to the regulation of apoptosis by cross-talk.

Also, 90 differentially expressed lncRNA (61 up-regulated and 29 down-regulated) were identified in our microarray assay. Pathway enrichment analysis identified a total of 6 significantly differential signaling pathways. Among them, inactivation of Cdc42 and Rac, signaling by the Robo receptor, Rho GTPase cycle, and PDGF signaling pathway has been previously reported to be associated with regulation of apoptosis. For example, both Cdc42 and Rac, subgroup members of Rho GTPases, suppressed apoptosis through the regulation of cell cycle progression[28, 30]. Moreover, the Robo receptor also has been reported to regulate various cellular processes, including cell proliferation, apoptosis, adhesion, and migration[29]. The PDGF family is divided into four subtypes: PDGF-A, PDGF-B, PDGF-C, and PDGF-D; of these, PDGF-D plays a key role in the regulation of proliferation, apoptosis, migration of cancer cells[31, 43] as well as apoptosis in hepatic stellate cells[44].

A CNC network constructed to investigate the interaction between differentially expressed mRNA and lncRNA in Dex-induced apoptosis of hBMSCs identified some key mRNAs, such as SAMHD1, CDK1,

GINS4, CDH11 and CIT, which were closely associated with regulation of cell proliferation and apoptosis. In addition, some important lncRNA identified included, ENSG00000233901.1, ENSG00000251018.2, ENSG00000255733.1, ENSG00000226605.1, ENSG00000233901.1, ENSG00000230921.1, SETMAR. Most importantly, there was a significant correlation between these key transcripts. For instance, GINS4 was positively correlated with ENSG00000251018.2, but negatively with ENSG00000233901.1. CDH11 was positively correlated with SETMAR, and negatively with ENSG00000230921.1. Besides, SAMHD1, CDK1,, and CIT were negatively correlated with ENSG00000255733.1, ENSG00000226605.1, and ENSG00000233901.1, respectively. Although the relationship between these lncRNAs involved in CNC network and apoptosis has not been previously reported, they may regulate apoptosis by interacting with mRNA, due to the correlation between them.

Next, we selected 6 differentially expressed mRNA and 4 differentially expressed lncRNA, which have been reported in previous studies, to confirm the reliability of the microarray data and facilitate further analysis. Gene expression analysis by qRT-PCR confirmed that both GINS4, CIT, and CDK1 were up-regulated, and BCL2-L11, SAMHD1, and CDH11 were down-regulated. Besides, lncRNAs STXBP5-AS1, IFNG-AS1, and MIR210HG were up-regulated, while ZFHX4-AS1 was down-regulated. GINS4, also known as SLD5, is an important player in the initial stages of DNA replication. Down-regulation of GINS4 promoted cell cycle arrest, growth inhibition, and apoptosis in colorectal cancer cells[32]. Inactivation of CIT, a serine/threonine kinase, increased apoptosis, suppressed proliferation, and arrested cell cycle via the regulation of Cyclophilin A in PDAC cells[33]. Similarly, inhibition of CDK1, a mitosis-promoting factor, promoted apoptosis of cancer cells through G_2/M arrest [34]. BCL2-L11, a member of the Bcl-2 family, was pro-apoptotic in cardiomyocytes due to its interaction with Bcl-2[45, 46]. SAMHD1, a mammalian dNTP hydrolase (dNTPase), increased apoptosis and reduced the proliferation of cancer cells by regulating the G_1/G_0 phase [35]. CDH11 belonging to the cadherin family induced apoptosis, inhibited cell proliferation by arresting cell cycle in the G_0/G_1 phase in colorectal cancer cell lines[36].

The lncRNA IFNG-AS1 has been reported to inhibit apoptosis, promote proliferation, invasion, and migration of HP75 cells [47]. Likewise, lncRNA ZFHX4-AS1 repressed apoptosis of breast cancer cells by regulating the Hippo signaling pathway[48]. In addition, the anti-apoptotic effects of MIR210HG in cancer cells by promoting proliferation and invasion in cervical cancer[49]. On the other hand, STXBP5-AS1 promoted apoptosis, suppressed proliferation, and invasion of MCF-7 cancer cells [50]. It can be stated that both mRNA (GINS4, CIT, and CDK1) and lncRNA (IFNG-AS1, ZFHX4-AS1, and MIR210HG) can be anti-apoptotic, whereas BCL2-L11, SAMHD1, and CDH11 and STXBP5-AS1 can be pro-apoptotic in specific cell lines. It is interesting to note that up-regulation of STXBP5-AS1 (apoptosis activators) and down-regulation of ZFHX4-AS1 (apoptosis inhibitors) in Dex-induced hBMSCs were consistent in both qRT-PCR and microarray analysis. Contrarily, the expression of the other 8 genes was inconsistent with the pro-apoptotic effect of Dex on hBMSCs. To our knowledge, the regulation of apoptotic genes is cell-type dependent. For instance, previous studies demonstrated that the lncRNA H19 inhibited MC apoptosis[51], but promoted apoptosis in cardiomyocytes and hippocampal neurons[52, 53]. Hence, given the cell-type

specificity of Dex induced responses, the roles and underlying mechanisms of the genes identified in the present study need further elucidation.

Collectively, we identified differentially expressed lncRNA and mRNA in Dex-induced apoptosis of hBMSCs by microarray. Bioinformatic analysis such as GO enrichment analysis, pathway enrichment analysis, and CNC network construction further revealed the role of these differentially expressed genes. The present study provides evidence in support of further studies to reveal the exact mechanisms of Dex-induced apoptosis of BMSCs.

5. Conclusions

Collectively, we utilized microarray to identify differentially expressed lncRNA and mRNA in Dex-induced apoptotic hBMSCs, and bioinformatics to explore the interaction between the differentially expressed genes. This study demonstrates the molecular mechanisms of Dex-induced apoptosis of hBMSCs and provides a new research direction for the study of the pathogenesis of steroid-induced osteonecrosis of femoral head.

Abbreviations

hBMSCs: Human bone marrow mesenchymal stem cells; Dex: Dexamethasone; GC: glucocorticoid; OP: osteoporosis; SONFH: steroid-induced osteonecrosis of the femoral head; lncRNAs: long noncoding RNAs; qRT-PCR: quantitative real-time PCR; THA: total hip arthroplasty; PBS: phosphate-buffered saline; ALP: alkaline phosphatase; GO: Gene ontology; CNC: coding-non-coding gene.

Declarations

Acknowledgements

Not applicable.

Funding

This study was supported by grants from the National Natural Science Foundation of China; Grant number: 81802151; Shandong Province Natural Science Foundation; Grant number: ZR2016HQ05, ZR2017BH089, ZR2019MH012; China Postdoctoral Science Foundation; Grant number: 2018M642616; Qingdao Applied Foundational Research Youth Project; Grant number: 19-6-2-55-cg.

Availability of data and materials

The datasets in current study are available from correspondence author on reasonable request.

Authors' contributions

Yingxing Xu: research method design, experiment operation, data analysis, and manuscript writing; Yingzhen Wang: experiment operation, data collection, and analysis; Tao Li and Yaping Jiang: human bone marrow tissues collection, research method design, manuscript revision.

Competing interests

The authors declare that they have no competing interests.

Consent for publication

Not applicable.

Ethical approval and consent to participate

The present study was approved by the Ethics Committee of the Affiliated Hospital of Qingdao University (Qingdao, China). All donors gave signed informed consent.

References

1. Uccelli A, Moretta L, Pistoia V. Mesenchymal stem cells in health and disease. Nat Rev Immunol. 2008;8:726–36.
2. Houdek MT, Wyles CC, Packard BD, Terzic A, Behfar A, Sierra RJ. Decreased osteogenic activity of mesenchymal stem cells in patients with corticosteroid-induced osteonecrosis of the femoral head. J Arthroplasty. 2016;31:893–8.
3. Yeung DK, Griffith JF, Antonio GE, Lee FK, Woo J, Leung PC. Osteoporosis is associated with increased marrow fat content and decreased marrow fat unsaturation: a proton MR spectroscopy study. J Magn Reson Imaging. 2005;22:279–85.
4. Hofbauer LC, Rauner M. Minireview: live and let die: molecular effects of glucocorticoids on bone cells. Mol Endocrinol. 2009;23:1525–31.
5. Song IH, Caplan AI, Dennis JE. Dexamethasone inhibition of confluence-induced apoptosis in human mesenchymal stem cells. J Orthop Res. 2009;27:216–21.
6. Fan Q, Zhan X, Li X, Zhao J, Chen Y. Vanadate inhibits dexamethasone-induced apoptosis of rat bone marrow-derived mesenchymal stem cells. Ann Clin Lab Sci. 2015;45:173–80 PubMed:25887871.
7. Wang HY, Pang B, Li Y, Zhu D, Pang TX, Liu YJ. Dexamethasone has variable effects on mesenchymal stromal cells. Cytotherapy. 2012;14:423–30.
8. Cárcamo-Orive I, Gaztelumendi A, Delgado J, Tejados N, Dorronsoro A, Fernández-Rueda J, Pennington DJ, Trigueros C. Regulation of human bone marrow stromal cell proliferation and differentiation capacity by glucocorticoid receptor and AP-1 crosstalk. J Bone Miner Res. 2010;25:2115–25.
9. Li X, Zhan J, Hou Y, Hou Y, Chen S, Luo D, Luan J, Wang L, Lin D. Coenzyme Q10 Regulation of Apoptosis and Oxidative Stress in H_2O_2 Induced BMSC Death by Modulating the Nrf-2/NQO-1

Signaling Pathway and Its Application in a Model of Spinal Cord Injury. Oxid Med Cell Longev. 2019;12:6493081.

10. Weinberg E, Maymon T, Weinreb M. AGEs induce caspase-mediated apoptosis of rat BMSCs via TNFα production and oxidative stress. J Mol Endocrinol. 2014;52(1):67–76.
11. Cai F, Hong X, Tang X, Liu NC, Wang F, Zhu L, Xie XH, Xie ZY, Wu XT. ASIC1a activation induces calcium-dependent apoptosis of BMSCs under conditions that mimic the acidic microenvironment of the degenerated intervertebral disc. Biosci Rep. 2019;39(11):BSR20192708.
12. Cheng XX, Yang QY, Qi YL, Liu ZZ, Liu D, He S, Yang LH, Xie J. Apoptosis of mesenchymal stem cells is regulated by Rspo1 via the Wnt/β-catenin signaling pathway. Chronic Dis Transl Med. 2019;5(1):53–63.
13. Patil VVS, Zhou R, Rana TM. Gene regulation by non-coding RNAs. Crit Rev Biochem Mol Biol. 2014;49:16–32.
14. Wei B, Wei W, Zhao B, Guo X, Liu S. Long non-coding RNA HOTAIR inhibits miR-17-5p to regulate osteogenic differentiation and proliferation in non-traumatic osteonecrosis of the femoral head. PLOS One. 2017;12:e0169097.
15. Huang Y, Zheng Y, Jia L, Li W. Long noncoding RNA H19 promotes osteoblast differentiation via TGF-beta1/Smad3/HDAC signaling pathway by deriving miR-675. Stem Cells. 2015;33:3481–92.
16. Otsuru S, Hofmann TJ, Olson TS, Dominici M, Horwitz EM. Improved isolation and expansion of bone marrow mesenchymal stromal cells using a novel marrow filter device. Cytotherapy. 2013;15:146–53.
17. Rosas M, Birkenkamp KU, Lammers JW, Koenderman L, Coffer PJ. Cytokine mediated suppression of TF-1 apoptosis requires PI3K activation and inhibition of Bim expression. FEBS Lett. 2005;579(1):191–8.
18. Kim YM, Chung HT, Kim SS, Han JA, Yoo YM, Kim KM, Lee GH, Yun HY, Green A, Li J, Simmons RL, Billiar TR. Nitric oxide protects PC12 cells from serum deprivation-induced apoptosis by cGMP-dependent inhibition of caspase signaling. J Neurosci. 1999;19(16):6740–7.
19. Verma S, Goyal S, Tyagi C, Jamal S, Singh A, Grover A. BIM (BCL-2 interacting mediator of cell death) SAHB (stabilized α helix of BCL2) not always convinces BAX (BCL-2-associated X protein) for apoptosis. J Mol Graph Model. 2016;67:94–101.
20. Slaymi C, Vignal E, Crès G, Roux P, Blangy A, Raynaud P, Fort P. The atypical RhoU/Wrch1 Rho GTPase controls cell proliferation and apoptosis in the gut epithelium. Biol Cell. 2019;111(5):121–41.
21. Dasgupta N, Thakur BK, Ta A, Das S, Banik G, Das S. Polo-like kinase 1 expression is suppressed by CCAAT/enhancer-binding protein α to mediate colon carcinoma cell differentiation and apoptosis. Biochim Biophys Acta Gen Subj. 2017;1861(7):1777–87.
22. Shirvan A, Ziv I, Machlin T, Zilkha-Falb R, Melamed E, Barzilai A. Two waves of cyclin B and proliferating cell nuclear antigen expression during dopamine-triggered neuronal apoptosis. J Neurochem. 1997;69(2):539–49.

23. Zou Z, Tao T, Li H, Zhu X. mTOR signaling pathway and mTOR inhibitors in cancer: progress and challenges. Cell Biosci. 2020;10:31.
24. Tian D, Li Y, Li X, Tian Z. Aloperine inhibits proliferation, migration and invasion and induces apoptosis by blocking the Ras signaling pathway in human breast cancer cells. Mol Med Rep. 2018;18(4):3699–710.
25. Zhao XL, Yu CZ. Vosaroxin induces mitochondrial dysfunction and apoptosis in cervical cancer HeLa cells: Involvement of AMPK/Sirt3/HIF-1 pathway. Chem Biol Interact. 2018;290:57–63.
26. Fang H, Li HF, Yang M, Liao R, Wang RR, Wang QY, Zheng PC, Zhang FX, Zhang JP. NF-κB signaling pathway inhibition suppresses hippocampal neuronal apoptosis and cognitive impairment via RCAN1 in neonatal rats with hypoxic-ischemic brain damage. Cell Cycle. 2019;18(9):1001–18.
27. Zhang Y, Alexander PB, Wang XF. TGF-β Family Signaling in the Control of Cell Proliferation and Survival. Cold Spring Harb Perspect Biol. 2017;9(4):a022145.
28. Selva E, Brest P, Loubat A, Lassalle S, Auberger P, Hofman P. Inhibition of apoptosis induced by heat shock preconditioning is associated with decreased phagocytosis in human polymorphonuclear leukocytes through inhibition of Rac and Cdc42. Immunol Cell Biol. 2007;85(3):257–64.
29. Zhang X, Li J, Liu J, Luo H, Gou K, Cui S. Prostaglandin F2α upregulates Slit/Robo expression in mouse corpus luteum during luteolysis. J Endocrinol. 2013;218(3):299–310.
30. Wang L, Shen S, Xiao H, Ding F, Wang M, Li G, Hu F. ARHGAP24 inhibits cell proliferation and cell cycle progression and induces apoptosis of lung cancer via a STAT6-WWP2-P27 axis. Carcinogenesis. 2019;20:bgz144.
31. Li P, Zhang Z, Zhang F, Zhou H, Sun B. Effects of 3-Tetrazolyl Methyl-3-Hydroxy-Oxindole Hybrid (THOH) on Cell Proliferation, Apoptosis, and G2/M Cell Cycle Arrest Occurs by Targeting Platelet-Derived Growth Factor D (PDGF-D) and the MEK/ERK Signaling Pathway in Human Lung Cell Lines SK-LU-1, A549, and A-427. Med Sci Monit. 2018;24:4547–54.
32. Rong Z, Luo Z, Zhang J, Li T, Zhu Z, Yu Z, Fu Z, Qiu Z, Huang C. GINS complex subunit 4, a prognostic biomarker and reversely mediated by Krüppel-like factor 4, promotes the growth of colorectal cancer. Cancer Sci. 2020;111(4):1203–17.
33. Cong L, Bai Z, Du Y, Cheng Y. Citron Rho-Interacting Serine/Threonine Kinase Promotes HIF1a-CypA Signaling and Growth of Human Pancreatic Adenocarcinoma. Biomed Res Int. 2020;2020:9210891.
34. Castedo M, Perfettini JL, Roumier T, Kroemer G. Cyclin-dependent kinase-1: linking apoptosis to cell cycle and mitotic catastrophe. Cell Death Differ. 2002;9(12):1287–93.
35. Bonifati S, Daly MB, St Gelais C, Kim SH, Hollenbaugh JA, Shepard C, Kennedy EM, Kim DH, Schinazi RF, Kim B, Wu L. SAMHD1 controls cell cycle status, apoptosis and HIV-1 infection in monocytic THP-1 cells. Virology. 2016;495:92–100.
36. Yuan S, Li L, Xiang S, Jia H, Luo T. Cadherin-11 is inactivated due to promoter methylation and functions in colorectal cancer as a tumour suppressor. Cancer Manag Res. 2019;11:2517–29.
37. Doi M, Nagano A, Nakamura Y. Genome-wide screening by cDNA microarray of genes associated with matrix mineralization by human mesenchymal stem cells in vitro. Biochem Biophys Res

Commun. 2002;290(1):381–90.

38. An S, Yang Y, Ward R, Liu Y, Guo XX, Xu TR. A-Raf: A new star of the family of raf kinases. Crit Rev Biochem Mol Biol. 2015;50(6):520–31.
39. Bellamy CO. p53 and Apoptosis. Br Med Bull. 1997;53(3):522–38.
40. Meng SS, Xu XP, Chang W, Lu ZH, Huang LL, Xu JY, Liu L, Qiu HB, Yang Y, Guo FM. LincRNA-p21 promotes mesenchymal stem cell migration capacity and survival through hypoxic preconditioning. Stem Cell Res Ther. 2018;9(1):280.
41. Hou J, Wang L, Wu Q, Zheng G, Long H, Wu H, Zhou C, Guo T, Zhong T, Wang L, Chen X, Wang T. Long noncoding RNA H19 upregulates vascular endothelial growth factor A to enhance mesenchymal stem cells survival and angiogenic capacity by inhibiting miR-199a-5p. Stem Cell Res Ther. 2018;9(1):109.
42. Li X, Wang J, Pan Y, Xu Y, Liu D, Hou Y, Zhao G. Long non-coding RNA HULC affects the proliferation, apoptosis, migration, and invasion of mesenchymal stem cells. Exp Biol Med (Maywood). 2018;243(13):1074–82.
43. Wang Z, Ahmad A, Li Y, Kong D, Azmi AS, Banerjee S, Sarkar FH. Emerging roles of PDGF-D signaling pathway in tumor development and progression. Biochim Biophys Acta. 2010;1806(1):122–30.
44. Wu X, Zhi F, Lun W, Deng Q, Zhang W. Baicalin inhibits PDGF-BB-induced hepatic stellate cell proliferation, apoptosis, invasion, migration and activation via the miR-3595/ACSL4 axis. Int J Mol Med. 2018;41(4):1992–2002.
45. Yang W, Han Y, Yang C, Chen Y, Zhao W, Su X, Yang K, Jin W. MicroRNA-19b-1 reverses ischaemia-induced heart failure by inhibiting cardiomyocyte apoptosis and targeting Bcl2 l11/BIM. Heart Vessels. 2019;34(7):1221–9.
46. Puthalakath H, O'Reilly LA, Gunn P, Lee L, Kelly PN, Huntington ND, Hughes PD, Michalak EM, McKimm-Breschkin J, Motoyama N, Gotoh T, Akira S, Bouillet P, Strasser A. ER stress triggers apoptosis by activating BH3-only protein Bim. Cell. 2007;129(7):1337–49.
47. Lu G, Duan J, Zhou D. Long-noncoding RNA lFNG-AS1 exerts oncogenic properties by interacting with epithelial splicing regulatory protein 2 (ESRP2) in pituitary adenomas. Pathol Res Pract. 2018;214(12):2054–61.
48. Li SY, Wang H, Mai HF, Li GF, Chen SJ, Li GS, Liang BC. Down-regulated long non-coding RNA RNAZFHX4-AS1 suppresses invasion and migration of breast cancer cells via FAT4-dependent Hippo signaling pathway. Cancer Gene Ther. 2019;26(11–12):374–87.
49. Wang AH, Jin CH, Cui GY, Li HY, Wang Y, Yu JJ, Wang RF, Tian XY. MIR210HG promotes cell proliferation and invasion by regulating miR-503-5p/TRAF4 axis in cervical cancer. Aging. 2020;12(4):3205–17.
50. Ham J, Jeong D, Park S, Kim HW, Kim H, Kim SJ. Ginsenoside Rg3 and Korean Red Ginseng extract epigenetically regulate the tumor-related long noncoding RNAs RFX3-AS1 and STXBP5-AS1. J Ginseng Res. 2019;43(4):625–34.

51. Hou J, Wang L, Wu Q, Zheng G, Long H, Wu H, Zhou C, Guo T, Zhong T, Wang L, Chen X, Wang T. Long noncoding RNA H19 upregulates vascular endothelial growth factor A to enhance mesenchymal stem cells survival and angiogenic capacity by inhibiting miR-199a-5p. Stem Cell Res Ther. 2018;9(1):109.
52. Zhang Y, Zhang M, Xu W, Chen J, Zhou X. The long non-coding RNA H19 promotes cardiomyocyte apoptosis in dilated cardiomyopathy. Oncotarget. 2017;8(17):28588–94.
53. Han CL, Ge M, Liu YP, Zhao XM, Wang KL, Chen N, Hu W, Zhang JG, Li L, Meng FG. Long non-coding RNA H19 contributes to apoptosis of hippocampal neurons by inhibiting let-7b in a rat model of temporal lobe epilepsy. Cell Death Dis. 2018;9(6):617.

Figures

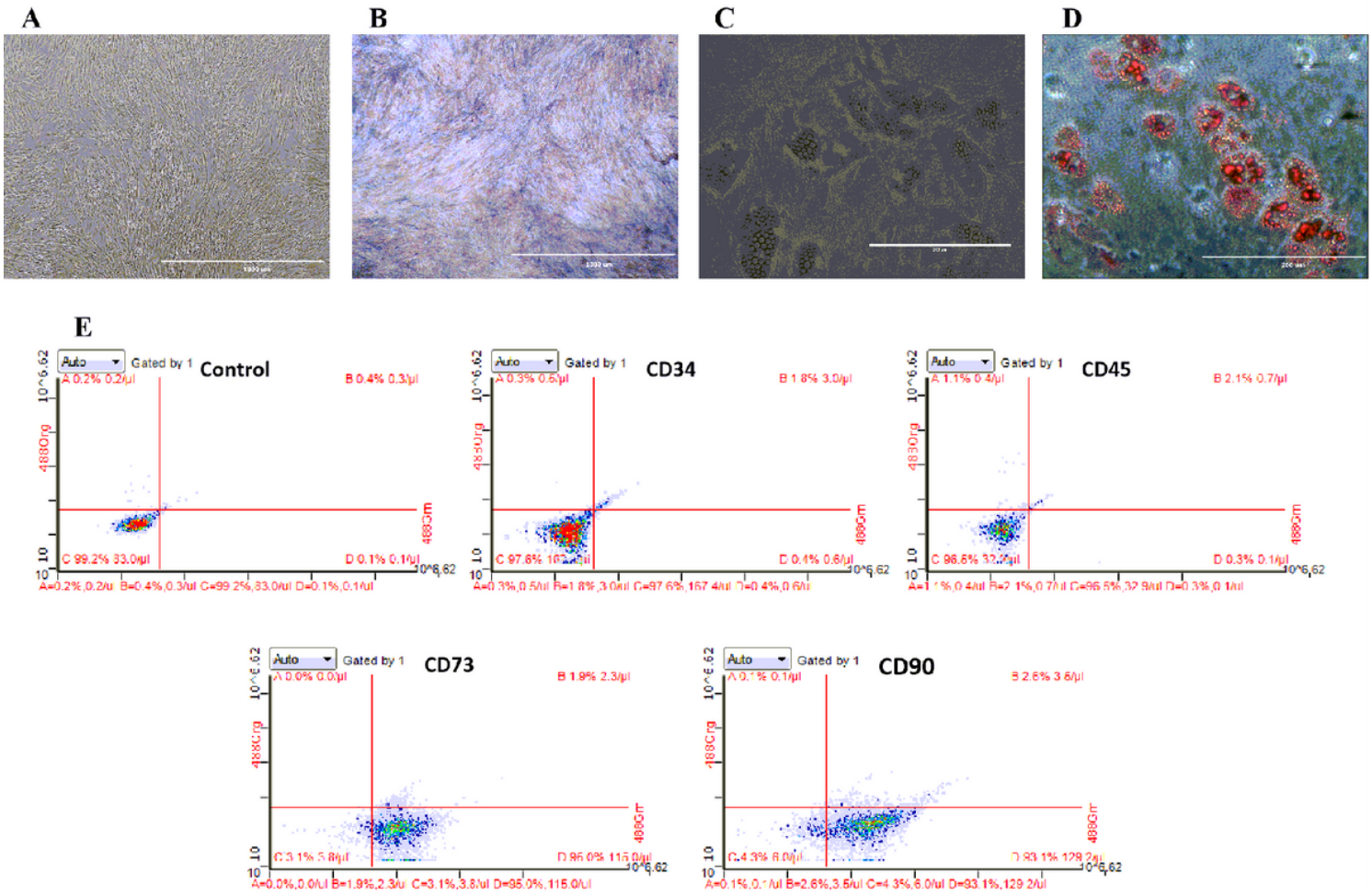

Figure 1

Identification of hBMSCs. (A) Representative images showing morphology of hBMSCs under an inverted phase contrast microscope (scale bar = 1000 um). (B) ALP staining (scale bar = 1000 um). (C) Lipid droplets formation (scale bar = 200 um). (D) Oil red O staining (scale bar = 200 um). (E) Phenotypic

analysis of hBMSCs by flow cytometry (CD34, CD45, CD73, CD90). hBMSCs = human bone marrow mesenchymal stem cells. ALP = alkaline phosphatase.

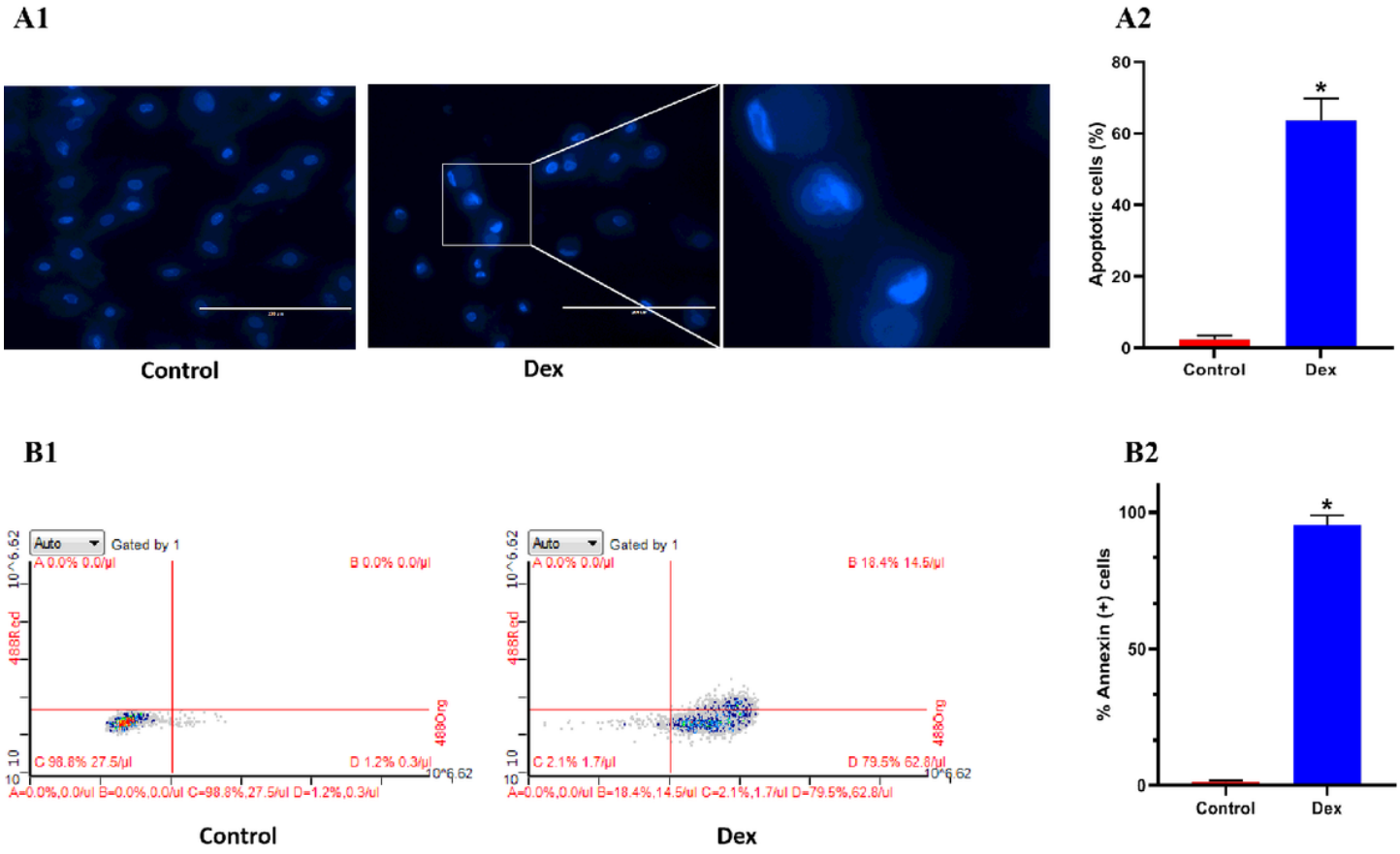

Figure 2

Dex-induced apoptosis of hBMSC. Hoechst 33342 staining showing (A1) apoptotic cells investigated under a fluorescence microscope (scale bar = 200 um), and (A2) percentage of apoptotic cells calculated by cell count. Flow cytometry showing (B1) apoptotic cells with Annexin V-PE and 7-AAD staining: Q1 representing necrotic cells, Q2 representing late apoptotic cells, Q3 representing normal cells, Q4 representing early apoptotic cells. (B2) percentage of Annexin+ cells in each group. Note: all data were presented as the mean value ± standard deviation of three independent experiments. *P < 0.05 compared with the control group. hBMSCs = human bone marrow mesenchymal stem cells, Dex = dexamethasone, Q = quadrant.

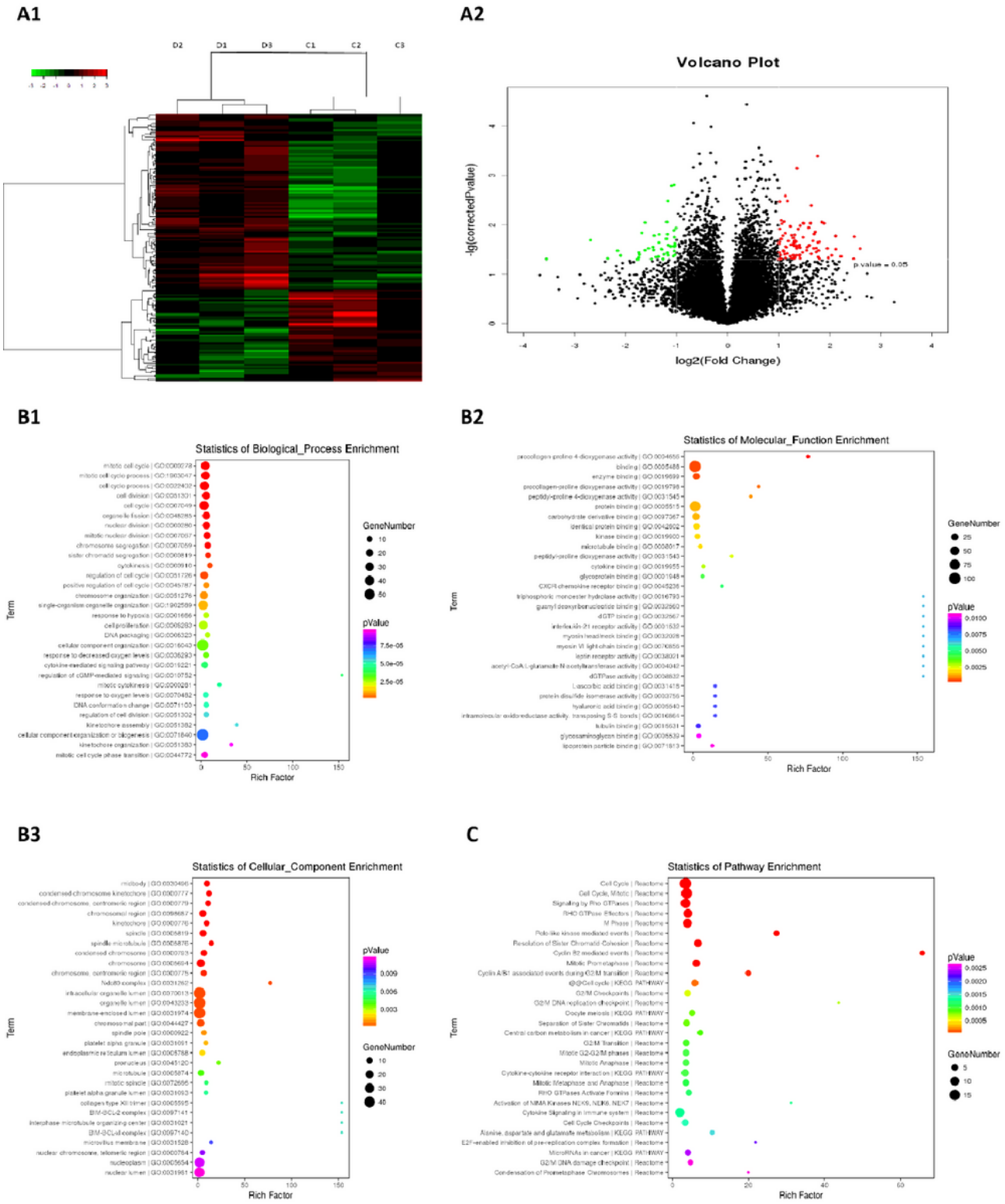

Figure 3

The differential expression profile of mRNA in Dex-induced apoptosis of hBMSCs and bioinformatic analysis. (A1) A heat map of distinct mRNA based on microarray assay. (A2) A volcano plot of distinct mRNA based on microarray assay-red dots represent up-regulation, and green dots represent down-regulation with statistical significance (fold change ≥2, P-value < 0.05). (B1) Bubble maps of GO enrichment analysis for biological process analysis. (B2) molecular function. (B3) cellular component

analysis. (C) A bubble map of pathway enrichment analysis showing the top 30 signaling pathways with significant changes. Notes: D = Dexamethasone-induced group (n = 3); C = Control group (n =3); Dex = dexamethasone; hBMSCs = human bone marrow mesenchymal stem cells; GO = gene ontology; KEGG = Kyoto Encyclopedia of Genes and Genomes pathway analysis.

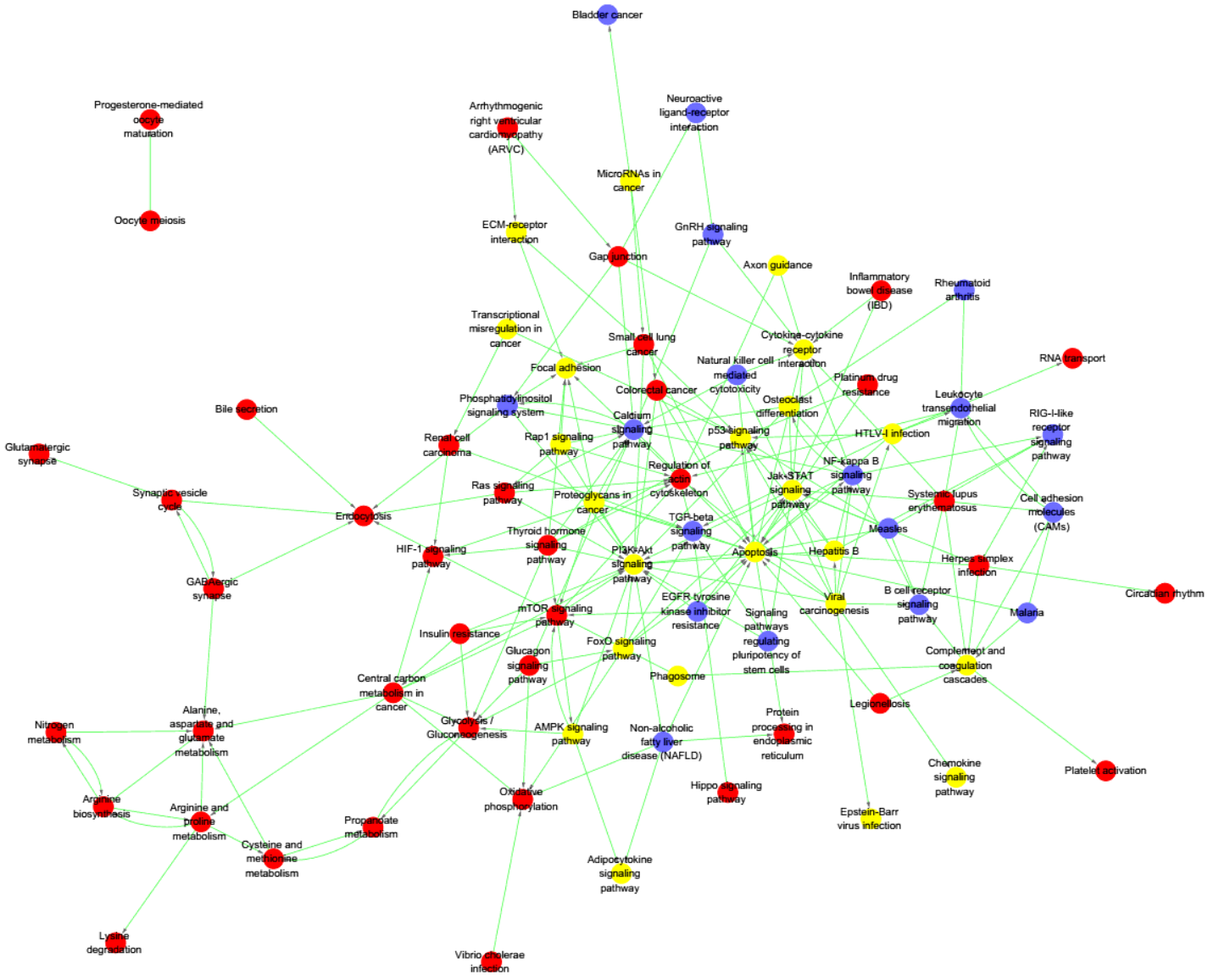

Figure 4

Interaction net of significant pathways (Path-Net) of the differential expression mRNA. Blue circle dots represent down-regulated pathways, red circle dots represent up-regulated pathways, and yellow circle dots represent up- and down-regulated pathways. The lines show interactions between pathways.

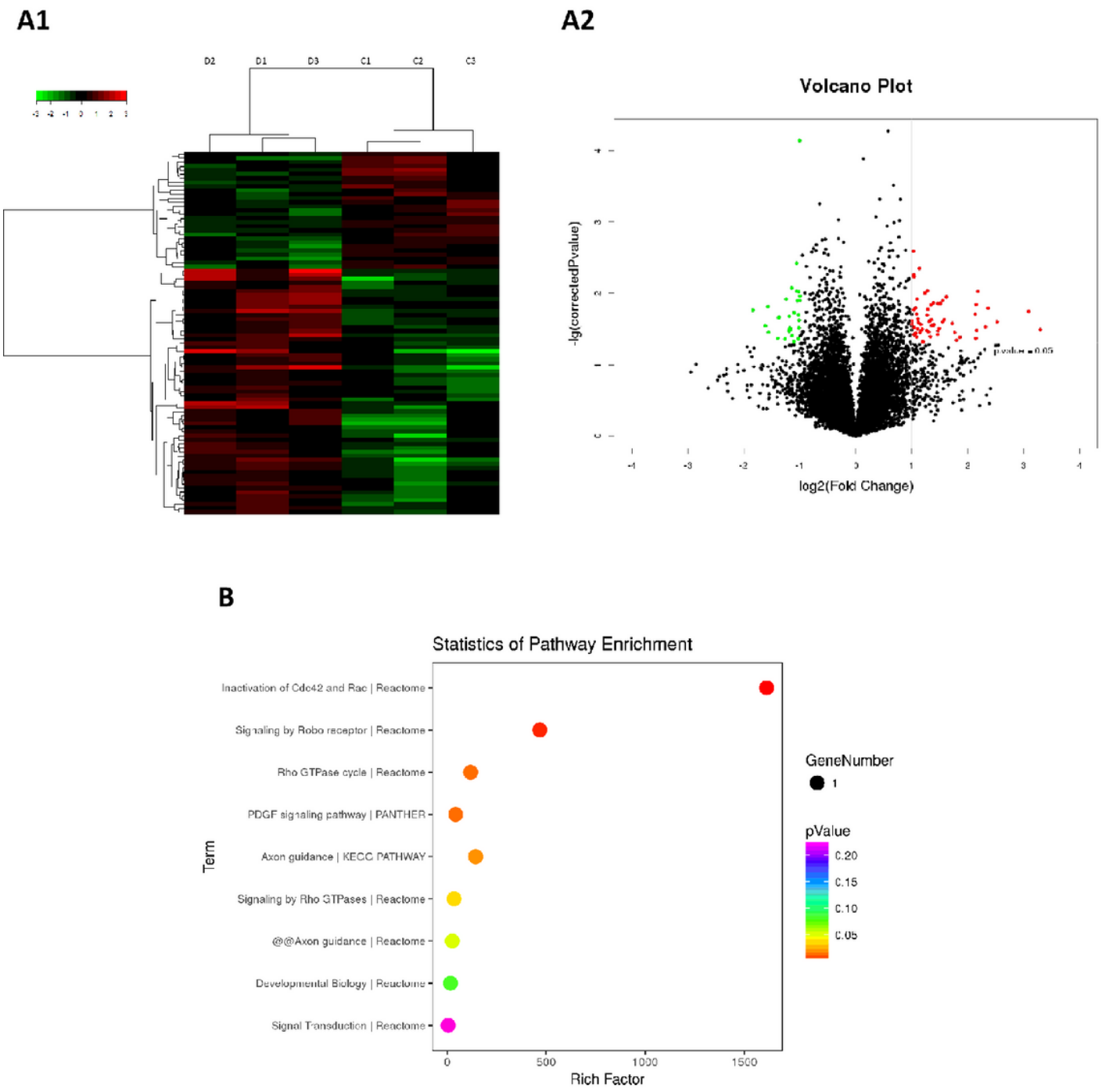

Figure 5

The differential expression profile of lncRNA in Dex-induced apoptosis of hBMSCs and bioinformatic analysis. (A1) A heat map of distinct lncRNA based on microarray assay. (A2) A volcano plot of distinct lncRNA based on microarray assay- red dots represent up-regulation, and green dots represent down-regulation of expression with statistical significance (fold change ≥2, P-value < 0.05). (B) A bubble map of pathway enrichment analysis. Notes: lncRNA = long noncoding RNA; D = Dexamethasone-induced group (n = 3); C = Control group (n =3); Dex = dexamethasone; hBMSCs = human bone marrow mesenchymal stem cells; KEGG = Kyoto Encyclopedia of Genes and Genomes pathway analysis.

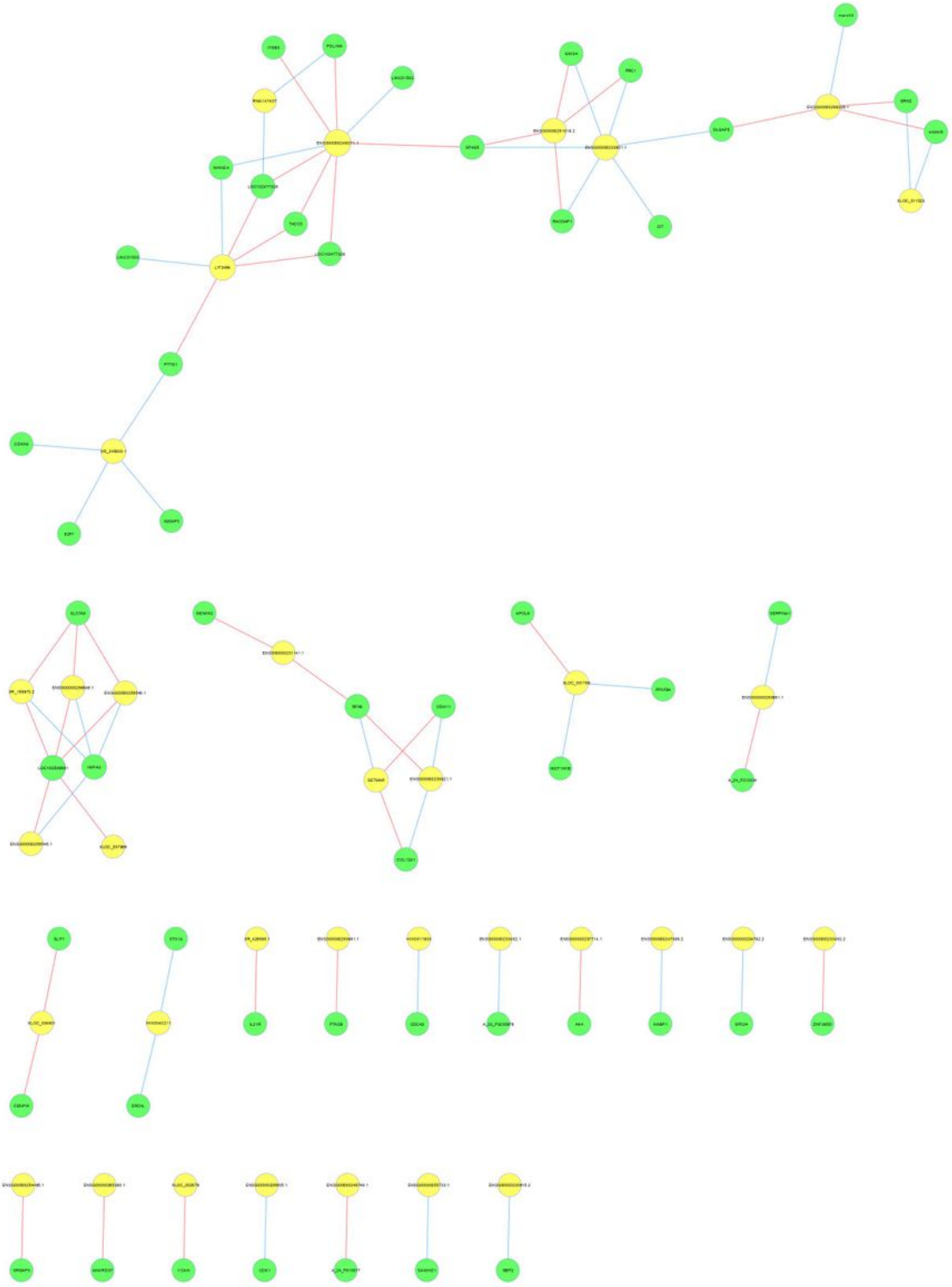

Figure 6

CNC network analysis of key differentially expressed mRNA and lncRNA. Yellow circle dots represent lncRNA, green circle dots represent mRNA. The size of the circle dot indicates the expression level of the gene. The lines show interactions between mRNA and lncRNA, red lines indicate positive and blue lines indicate a negative correlation. Notes: CNC = coding and noncoding; lncRNA = long noncoding RNA.

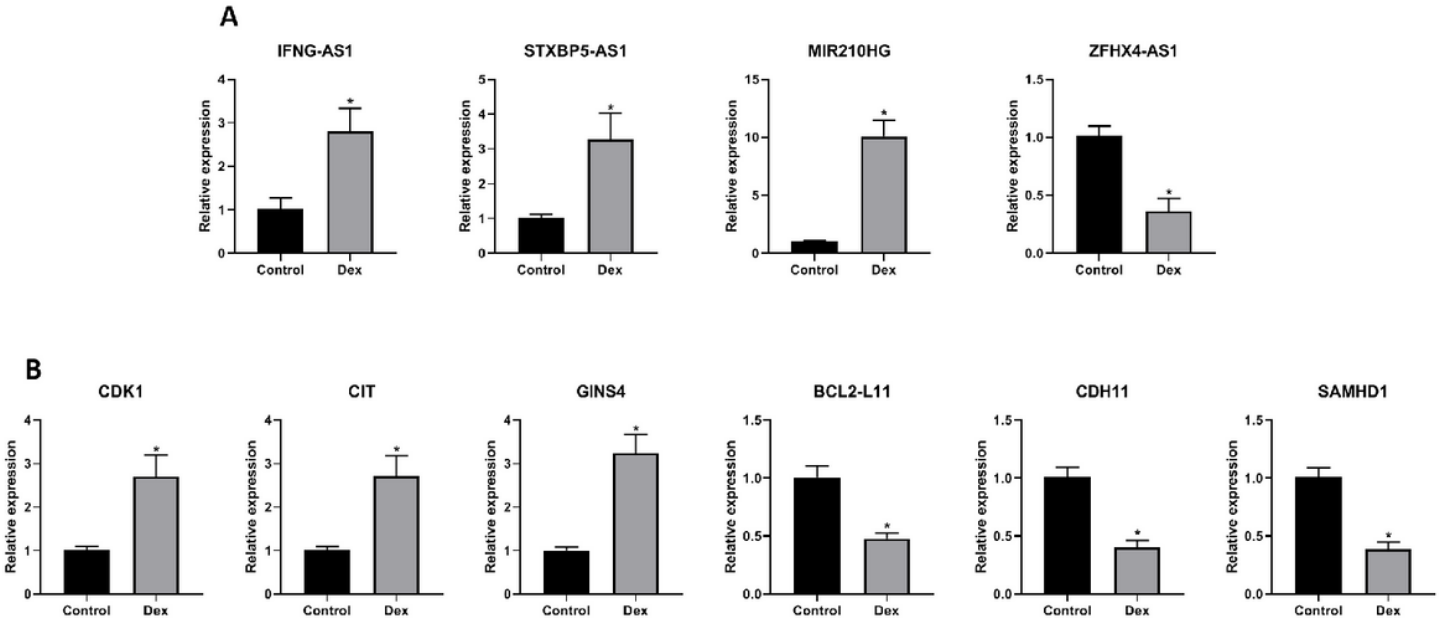

Figure 7

Confirmation of differentially expressed mRNA and lncRNA by qRT-PCR. Note: all data were presented as mean ± standard deviation of three independent experiments. *P < 0.05 compared with the control group. Dex = Dexamethasone-induced group; Control = Control group; lncRNA = long noncoding RNA; qRT-PCR = quantitative real time polymerase chain reaction; CIT = citron rho-interacting serine/threonine kinase; CDK1 = cyclin-dependent kinase 1; GINS4 = GINS complex subunit 4; BCL2-like 11 = B-cell lymphoma 2-Like 11; CDH11 = cadherin 11; SAMHD1 = SAM domain and HD domain 1.

Supplementary Files

This is a list of supplementary files associated with this preprint. Click to download.

- supplement12.xls
- supplement13.xlsx
- supplement14.xlsx